Effect of spatiotemporal variation of rainfall on dissolved oxygen depletion in integrated catchment studies

Antonio Manuel Moreno Ródenas[1, *], Francesca Cecinati[2], Marie-Claire ten Veldhuis[1], Jeroen Langeveld[1, 3] and François Clemens[1, 4]

[1]Technische Universiteit Delft, Water Management Department, The Netherlands
(*Email: *a.m.morenorodenas@tudelft.nl)*
[2]University of Bristol, Department of Civil Engineering, UK
[3]Partners4urbanwater, Nijmegen, The Netherlands
[4]Deltares, Delft, The Netherlands

Keywords
Integrated Catchment Modelling; water quality; rainfall spatiotemporal variability; Geostatistics

This study addresses the effect of spatial and temporal resolution of rainfall fields on the performance of a simplified integrated catchment model for predicting dissolved oxygen concentrations in a river. For that purpose we propose a procedure to generate rainfall products with increasing spatial information at different time step accumulations (10', 30' and 60') at the spatial support of lumped urban catchment systems. Using a rain gauge network and single-polarization C-Band Radar data we generate 4 rainfall products; 1) Homogeneous rainfall from a single rain gauge, 2) Block kriging interpolation from a network of 13 rain gauges, 3) Averaged Radar estimation and 4) Universal block kriging from a rain gauge network and using Radar as an external covariate. Comparison of the model predictions with monitoring data in the river showed a low sensitivity to the temporal scales proposed and a relative improvement with increasing spatial information linked to the climatological characteristics of the storm period.

1 INTRODUCTION

The approval of the Water Framework Directive (WFD, 2000/60/EC 200) in the European Union enforces member states to reach a "good ecological and chemical status in inland and coastal water bodies". Several highly urbanised river systems across Europe still do not match the targeted water quality status, and complying with the environmental standards will require the adoption of intensive investment plans and regulatory measures. Integrated catchment models (ICM) are used as tools for decision support in this process, aiming to simulate the interaction between urban sewer networks, water treatment facilities and receiving waters (FWR, 2012). Fast and robust models are required in order to perform long-term scenario analysis and system optimization (Benedetti et al., 2012; Langeveld et al., 2013). Those modelling strategies are being increasingly proposed in operational and research cases. However, there is little knowledge on the requirements of rainfall data and its influence on the model performance.

In the modelled system, rainfall runoff fills the sewer system of urban areas located along the river. When flow exceeds the sewer infrastructure capacity, CSO structures (and storm settling tanks) discharge into the receiving water body. Depending on the magnitude of the emission and the buffer capacity of the river, this results in a degradation of the water quality status. Convective storms in the summer season couple various critical conditions; high rainfall intensities along with high temperatures and a low river base flow. In many urbanised river catchments, distances between municipal areas are beyond the de-correlation length of convective storm processes (Bruni et al., 2015), meaning that spatial and temporal scales provided by the rainfall input are possibly affecting the system's behaviour. Most reliable rainfall data measurements (well calibrated and maintained rain gauges) are often not sufficiently dense to adequately represent the spatial variation of rainfall. The use of additional rainfall data, like weather radar and municipal rain gauge networks can provide additional spatial information, at a cost of a higher uncertainty of the measured input.

This study investigates the effect of accounting for increasingly detailed spatiotemporal rainfall data in the performance of a *simplified integrated catchment model* for predicting dissolved oxygen concentration in the river medium.

2 METHODS & MATERIALS

The study area is contributing to the Dommel, a relatively small river flowing through the city of Eindhoven (The Netherlands). This river section receives the discharge of a 750,000 p.e. waste water treatment plant (WWTP) and from over 200 combined sewer overflow structures. This system configuration produces common oxygen depletion events in which the river ecosystem is put under stress. A pseudo-distributed simplified water quality model was developed in WEST (mikedhi.com), more information can be found in Langeveld et al. (2013). This accounts for: the sewer processes at the draining municipalities, WWTP dynamics and the river tributaries, constituting a fully integrated system. **Figure 1** provides a scheme of the system's structure and measurement locations.

Figure 1 Location and structure of the catchment, rain gauges, monitoring station and radar position.

Local rainfall data were obtained from different sources across an area of 570km^2; automatic KNMI rain gauges produce the most reliable source of information (with 1 inside the catchment boundary, and 6 in the surrounding areas), a secondary network of 6 rain gauges managed by the Waterboard de Dommel and the municipality of Eindhoven provide extra spatial information within the urban catchment scales. Radar rainfall estimates from the KNMI composite can be obtained with a resolution of 1km^2 and 5 minutes. Rainfall inputs were generated by a dedicated geostatistical approach, rendering 4 rainfall input types with increasing spatial detail: 1) 1 homogeneous KNMI rain gauge, 2) Block kriging from the interpolation of 13 rain gauges (KNMI + Waterboard de Dommel), 3) Spatial average of the KNMI calibrated Radar and 4) Universal block kriging of 13 rain gauges using KNMI Radar as a covariate. Those products were accumulated at different timescales ranging from 10' to 1h. Three periods from the summer of 2011, 2012 and 2013 were simulated, which duration can be checked in the **Table 1**.

2.2 Rainfall characterisation

Convective storm processes present short spatial and temporal scales. Thus a denser measurement network would be required to fully capture its characteristics. Stratiform rainfall structures in the other hand show a more homogeneous intensity distribution. In order to identify the spatial structure of the rainfall processes studied we used the empirical semivariogram, which provides information on the relative de-correlation of the variable with increasing distance:

$$\hat{\gamma}(\boldsymbol{h}) = \frac{1}{2\left|N(\boldsymbol{h})\right|} \sum_{(i,j)\in N(h)} \left|R_i - R_j\right|^2 , \tag{1.1}$$

being $N(h)$ the number of sampled pairs located at a distance h, and R the variable measured at locations i and j. We assume stationarity of the rainfall field at any snapshot considered (in the selected accumulation time step). Additionally, due to the very limited density of punctual measurements, the rain field was considered isotropic and the semivariogram was computed as time-lumped, obtaining an averaged structure for each period considered. An exponential experimental semivariogram structure was fitted to the 1 km binned empirical one:

$$\gamma(\boldsymbol{h}) = \begin{cases} 0 & if\ |\boldsymbol{h}| = 0 \\ c_0 + c\left(1 - e^{-\frac{3|\boldsymbol{h}|}{\phi}}\right) & if\ |\boldsymbol{h}| > 0 \end{cases} , \tag{1.2}$$

where c is the partial sill, c_0 is the nugget effect and ϕ effective range or decorrelation distance (distance at which the semivariogram value reaches the 95% of the total sill). In this application no nugget effect was used, as van de Beek et al. (2012) didn't found a relevant nugget in rainfall processes in Netherlands even for short temporal scales. The information contained in the rain gauge measurement data was therefore assumed perfect, although this is not true in reality and the effect of the uncertainty of the individual rain gauge measurements should to be further studied.

Table 1 presents the parameter values fitted to the empirical semivariogram from the 13 rain gauge stations. The effective range gives information on the characteristic spatial scales of the period study at a given accumulation time step in minutes.

Table 1 Fitted parameters for an exponential semivariogram model.

	Period 1 10/08/2011 – 31/08/2011		Period 2 05/07/2012 – 04/08/2012		Period 3 25/07/2013 – 19/08/2013	
Time step (min)	Sill	Range [km]	Sill	Range [km]	Sill	Range [km]
10’	5.10	37.12	2.09	8.61	1.90	59.81
30’	2.11	35.39	1.00	15.00	0.82	55.78
60’	1.05	38.47	0.61	17.18	0.51	92.88

2.3 Rainfall products

The ICM considered in this application presents a simplified hydrological model structure for the rainfall-runoff and sewer routing dynamics of each municipality. This lumps spatially the processes at the municipality scale yet preserving the relative location of each individual system. To this effect the areas connected to municipality sewer systems were mapped and georeferenciated. Rainfall products were then generated in the spatial support of the subcatchment areas. This generated a total of 29 rainfall inputs for each product, time accumulation and period considered. It is worth to mention that the prediction of the averaged rainfall value in the catchment-area spatial support has a considerably lower predictive uncertainty than punctual estimations.

2.3.1 Single rain gauge (BK1)

The most reliable rain gauge in the area is KNMI_370. As shown in **Figure 1** it is located in the western part of the catchment, inside the Eindhoven airport. KNMI automatic rain gauges use a floating device and an electronic register, providing a high measuring frequency and resolution (1 min - 0.02 mm/h). The stations are calibrated and maintained regularly.

Therefore the KNMI_370 rain gauge was selected to generate homogeneous rainfall fields, simulating the case in which data is only present at a single location inside the catchment area. This, still being a reliable and accurate measurement for its punctual location, lacks of any spatial information, hence its validity will progressively deteriorate with the distance.

2.3.2 Block kriging of n rain gauges (Bkall)

Extra rainfall data was obtained in the area. Six tipping bucket rain gauges belonging to the municipality of Eindhoven and the Waterboard de Dommel are within the boundaries of the urban catchment. Six additional KNMI stations can be found in the surrounding area. Combined with the previous station, this provided a network of 13 punctual sampling points. In order to extend this information to unsampled locations we applied a block kriging procedure. Producing the best unbiased predictor on the spatial support of each urban catchment area.

2.3.3 Averaged radar quantitative estimation (ARadar)

The composite product of Radar from the KNMI was averaged in the areas of interest. This is a quantitative estimation of rainfall from the 2 C-Band Radars of Netherlands. The estimated field has been further bias-corrected by the KNMI in order to eliminate the systematic underestimation from raw Radar data (Overeem et al., 2009).

2.3.4 Universal block kriging rain gauge – radar

Weather radar is known to provide a good estimation of the rainfall field structure, however the punctual values often differ considerably in absolute value with the observed at ground level. On the other hand rain gauges generate accurate local measurements, although the low spatial coverage of rain gauge measurements generates a poor representation of the rainfall field at distant unsampled points. It is widely accepted that merging those punctual and distributed measurements can provide more accurate rainfall fields (Haberlandt, 2007; Overeem et al., 2009; Velasco-Forero et al., 2009). In this case we used a universal block kriging procedure. This uses the punctual rain gauge value to generate estimates at the catchment spatial support adapting the field to match external covariates (Radar estimates). This is an equivalency of kriging with external drift with outputs at block support.

3 RESULTS

We contrast the ICM simulations (using the different rainfall products) against monitoring data from the system. A graphical example of this comparison can be found in the **Figure 2**, where the relative match between the model and the monitored is shown for hourly-accumulated rainfall.

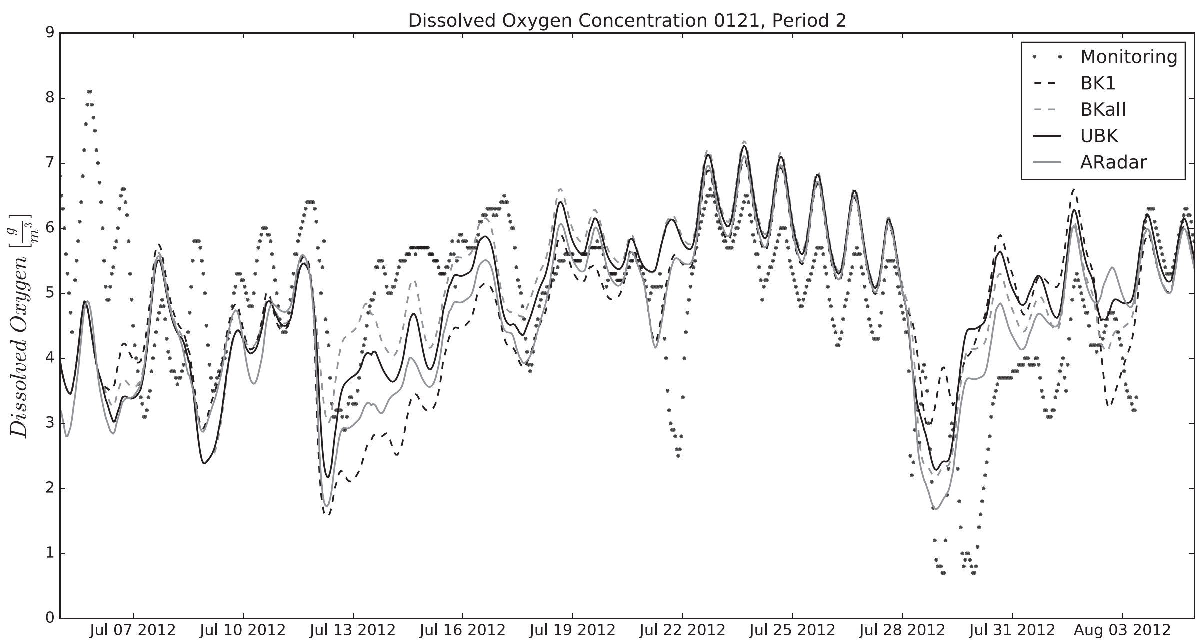

Figure 2 Dissolved oxygen concentration modelled using the different rainfall products at 60' accumulation and the monitoring station at the end of the catchment (roughly 17 km from the WWTP).

The results are summarized based in the following criteria; first we present the match between the dissolved oxygen concentration predictions and the monitoring time series using the Nash-Sutcliffe coefficient (Table 2) and the root mean squared error (Table 3).

Table 4 shows the absolute difference between the deepest drop of the period in the modelled and monitored time series. The objective of this kind of simplified model structures is not to match the dynamics to the perfection, but to be able to represent the consequences of the processes. In water quality studies tables of frequency-intensity-duration of variable concentrations are extracted from natural species survival tolerances. This criterion attends to the capability of matching the intensity of depletion shown in monitoring data.

Table 2 Nash-Sutcliffe coefficient for modelled-monitored dissolved oxygen in the river section 0121

	Storm period 1, 10/08/2011 – 31/08/2011				Storm period 2 05/07/2012 – 04/08/2012				Storm period 3 25/07/2013 – 19/08/2013			
	BK1	BKall	ARadar	UBK	BK1	BKall	ARadar	UBK	BK1	BKall	ARadar	UBK
10’	-0.09	0.39	0.43	0.54	-0.26	-0.03	0.00	-0.01	0.20	0.18	-0.03	0.19
30’	-0.10	0.44	0.44	0.54	-0.28	0.03	-0.02	-0.10	0.19	0.18	-0.03	0.21
60’	-0.08	0.46	0.44	0.54	-0.29	0.05	-0.03	-0.07	0.20	0.19	-0.03	0.20

Table 3 RMSE for modelled-monitored dissolved oxygen in the river section 0121

	Storm period 1, 10/08/2011 – 31/08/2011				Storm period 2 05/07/2012 – 04/08/2012				Storm period 3 25/07/2013 – 19/08/2013			
	BK1	BKall	ARadar	UBK	BK1	BKall	ARadar	UBK	BK1	BKall	ARadar	UBK
10’	1.28	0.96	0.92	0.83	1.41	1.27	1.26	1.26	1.13	1.15	1.29	1.14
30’	1.28	0.92	0.91	0.83	1.42	1.23	1.27	1.32	1.14	1.15	1.29	1.13
60’	1.27	0.90	0.92	0.83	1.43	1.22	1.27	1.30	1.13	1.14	1.29	1.14

Table 4 Absolute difference between maximun drop of dissolved oxygen in modelled-monitored time series.

	Storm period 1, 10/08/2011 – 31/08/2011				Storm period 2 05/07/2012 – 04/08/2012				Storm period 3 25/07/2013 – 19/08/2013			
	BK1	BKall	ARadar	UBK	BK1	BKall	ARadar	UBK	BK1	BKall	ARadar	UBK
10’	1.45	1.28	1.21	1.10	2.15	1.76	0.88	1.39	1.19	1.33	1.48	1.28
30’	1.45	1.21	1.19	1.09	2.16	1.49	0.89	1.71	1.16	1.22	1.45	1.34
60’	1.45	1.16	1.18	1.10	2.15	1.38	0.88	1.48	1.13	1.13	1.40	1.28

4 CONCLUSIONS

In this study we describe the procedure of generating rainfall products using commonly available rainfall data at different spatial and temporal scales. We tested their effect on an integrated catchment model for dissolved oxygen concentrations predictions. It has been observed that dissolved oxygen outputs are not sensitive to the accumulated time steps considered (10, 30, 60 minutes) for the periods evaluated and for every spatial scale. This can be explained by the large delay in the hydraulic and biochemical processes in the system. Several studies have assessed the effect of spatiotemporal representation of rainfall in the hydrodynamic behaviour of urban drainage systems concluding that short temporal scales are relevant for matching flow patterns (Ochoa-Rodriguez et al., 2015). However, in the case of modelling dissolved oxygen concentrations the spilled and drained volumes are more relevant, which are less affected by the range of temporal scales considered. Furthermore when considering the effect of multiple individual drainage systems coupled in the same integrated system this effect further dissipates.

Regarding spatial scales, the results obtained show that increasing spatial information in the rainfall produces more accurate estimates. In general terms UBK slightly improves the performance of the model, being closely followed by the averaged Radar. The interpolation methods used in this application present a high sensitivity to failures in the rain gauge datasets. Thus the correct assessment of their quality or the inclusion of an error structure could further improve their performance. The use of a single rain gauge is not recommended, especially in the case of more convective cases as in the Storm period 2, since the shorter decorrelation lengths of rainfall can reach the distance between the different urban drainage systems. However it can still produce comparable results for more homogeneous rainfall processes as seen in the Storm period 3.

The model is not matching perfectly the measured time series as shown by the low Nash-Shutcliffe coefficients, but it can reproduce with relative accuracy the intensity of oxygen drops and the behaviour of the variable in storm conditions which is a relevant process for a water quality assessment target. This is accomplished with a very simplified structure confronted with datasets outside calibration conditions. However, necessary changes in the model structure have been observed specially to match the recovery pattern of dissolved oxygen concentrations and to match storm flow dynamics in the river system. Nevertheless those processes do not likely affect the conclusions found in this study.

Further work will focus on defining the characteristic spatial-temporal scales from the integrated urban water system in order to be compared with the climatological ones. This will help to characterise the required spatial information in the rainfall input data for any given case study.

5 ACKNOWLEDGEMENTS

This project has received funding from the European Union’s Seventh Framework Programme for research, technological development and demonstration under grant agreement no 607000. The authors would like to thank the KNMI, the Waterschap De Dommel, and the municipality of Eindhoven. Special thanks to Filip H.A. Claeys from DHI and to L. Benedetti for their counsel and advice in the WEST modelling platform.

6 REFERENCES

Benedetti, L., Batstone, D. J., De Baets, B., Nopens, I., & Vanrolleghem, P. A. (2012). Uncertainty analysis of WWTP control strategies made feasible. *Water Quality Research Journal of Canada, 47*(1), 14. doi: 10.2166/wqrjc.2012.038

Bruni, G., Reinoso, R., van de Giesen, N. C., Clemens, F. H. L. R., & ten Veldhuis, J. A. E. (2015). On the sensitivity of urban hydrodynamic modelling to rainfall spatial and temporal resolution. *Hydrology and Earth System Sciences, 19*(2), 691-709. doi: 10.5194/hess-19-691-2015

FWR. (2012). *Manual, Urban Polution Management* (3th ed.).

Haberlandt, U. (2007). Geostatistical interpolation of hourly precipitation from rain gauges and radar for a large-scale extreme rainfall event. *Journal of Hydrology, 332*(1-2), 144-157. doi: 10.1016/j.jhydrol.2006.06.028

Langeveld, J. G., Benedetti, L., de Klein, J. J. M., Nopens, I., Amerlinck, Y., van Nieuwenhuijzen, A., . . . Weijers, S. (2013). Impact-based integrated real-time control for improvement of the Dommel River water quality. *Urban Water Journal, 10*(5), 312-329. doi: 10.1080/1573062x.2013.820332

Ochoa-Rodriguez, S., Wang, L.-P., Gires, A., Pina, R. D., Reinoso-Rondinel, R., Bruni, G., . . . ten Veldhuis, M.-C. (2015). Impact of spatial and temporal resolution of rainfall inputs on urban hydrodynamic modelling outputs: A multi-catchment investigation. *Journal of Hydrology, 531*, 389-407. doi: 10.1016/j.jhydrol.2015.05.035

Overeem, A., Holleman, I., & Buishand, A. (2009). Derivation of a 10-Year Radar-Based Climatology of Rainfall. *Journal of Applied Meteorology and Climatology, 48*(7), 1448-1463. doi: 10.1175/2009jamc1954.1

van de Beek, C. Z., Leijnse, H., Torfs, P. J. J. F., & Uijlenhoet, R. (2012). Seasonal semi-variance of Dutch rainfall at hourly to daily scales. *Advances in Water Resources, 45*, 76-85. doi: 10.1016/j.advwatres.2012.03.023

Velasco-Forero, C. A., Sempere-Torres, D., Cassiraga, E. F., & Jaime Gómez-Hernández, J. (2009). A non-parametric automatic blending methodology to estimate rainfall fields from rain gauge and radar data. *Advances in Water Resources, 32*(7), 986-1002. doi: 10.1016/j.advwatres.2008.10.004